Ice-COLD-PCR enables rapid amplification and robust enrichment for low-abundance unknown DNA mutations

Coren A. Milbury[1,2], Jin Li[1,2] and G. Mike Makrigiorgos[1,2,*]

[1]Department of Radiation Oncology, Division of Medical Physics and Biophysics and [2]Department of Radiation Oncology, Division of DNA Repair and Genome Stability, Dana Farber-Brigham and Women's Cancer Center, Harvard Medical School, Boston, MA 02115, USA

ABSTRACT

Identifying low-abundance mutations within wild-type DNA is important in several fields of medicine, including cancer, prenatal diagnosis and infectious diseases. However, utilizing the clinical and diagnostic potential of rare mutations is limited by sensitivity of the molecular techniques employed, especially when the type and position of mutations are unknown. We have developed a novel platform that incorporates a synthetic reference sequence within a polymerase chain reaction (PCR) reaction, designed to enhance amplification of unknown mutant sequences during COLD-PCR (CO-amplification at Lower Denaturation temperature). This new platform enables an Improved and Complete Enrichment (ice-COLD-PCR) for all mutation types and eliminates shortcomings of previous formats of COLD-PCR. We evaluated ice-COLD-PCR enrichment in regions of TP53 in serially diluted mutant and wild-type DNA mixtures. Conventional-PCR, COLD-PCR and ice-COLD-PCR amplicons were run in parallel and sequenced to determine final mutation abundance for a range of mutations representing all possible single base changes. Amplification by ice-COLD-PCR enriched all mutation types and allowed identification of mutation abundances down to 1%, and 0.1% by Sanger sequencing or pyrosequencing, respectively, surpassing the capabilities of other forms of PCR. Ice-COLD-PCR will help elucidate the clinical significance of low-abundance mutations and our understanding of cancer origin, evolution, recurrence-risk and treatment diagnostics.

INTRODUCTION

Identifying low-abundance mutations is important in several fields of medicine, including cancer, prenatal diagnosis and infectious diseases (1–3). For example, in clinical samples from infiltrating and multi-focal cancer types, mutation-containing cancer cells are greatly outnumbered by an excess of normal cells (4–6). Yet it is often very important to identify such mutational 'needles in a haystack'. Low-abundance DNA mutations in heterogeneous specimens from precancerous or cancerous tissue biopsies, sputum, urine, stool or circulating DNA released in blood can cause drug resistance and can be clinically significant biomarkers (7). However, utilizing the clinical and diagnostic potential of such rare mutations is often limited by accuracy and sensitivity of the molecular techniques and methods employed. The polymerase chain reaction (PCR) is the foundation of most molecular applications that investigate DNA sequence variation. Several methods can enrich low-abundance mutations at pre-determined positions during PCR amplification (8). However, when the position and type of such mutations on the DNA sequence is unknown there are very few approaches that can enrich mutations such that they can be identified by downstream technologies (8).

CO-amplification of major and minor alleles at Lower Denaturation temperature [COLD-PCR (9)] is a recently developed PCR approach capable of enriching low-abundance mutants at any position on the sequence. COLD-PCR operates by incorporating a critical denaturation temperature (T_c) for a given DNA sequence. At the T_c, the percent of amplicons that denature is dependent on the exact melting properties of the interrogated DNA sequence, thereby single point mutations or micro-deletions influence substantially the balance of the resulting single and double-stranded DNA molecules. In COLD-PCR, the T_c and cycling employed is such that

mutation-containing sequences end up in double-stranded DNA molecules that denature preferentially over wild-type (WT) duplexes, by means of their reduced melting temperature. Accordingly, mutation-containing sequences become preferentially amplified during amplification. This simple principle enables COLD-PCR to amplify mutation-containing alleles with a several-fold selectivity over WT alleles (9). Advantages of COLD-PCR include its relative simplicity, the preferential amplification of mutant-containing DNA without the need for cumbersome protocols or additional reagents, and the ability to subsequently sequence the amplified product and identify the mutation. COLD-PCR can be used in place of conventional PCR and combined with most downstream assays, yet it requires little to no additional cost, time and labor. Mutation detection sensitivities have been improved several-fold by combining COLD-PCR with established downstream applications such as Sanger sequencing (9–11), dHPLC analysis (9); MALDI-TOF (9), Pyrosequencing (9), real-time TaqMan PCR (12), SSCP (13), mutation-specific restriction enzyme digestion (14) and high resolution melting (10,15).

Although the applications of COLD-PCR in DNA diagnostics are proliferating (8,16) there are still disadvantages in the technology as currently applied. Depending upon the type of mutation that is of interest or the degree of mutation enrichment required, COLD-PCR is currently applied in either of two formats: *full*-COLD-PCR or *fast*-COLD-PCR (9). *Full*-COLD-PCR enriches all possible mutations along the sequence, though the enrichment of mutation-containing sequences relative to wild type sequences is generally modest (3- to 10-fold) relative to *fast*-COLD-PCR. Furthermore, in *full*-COLD-PCR, several minutes of an intermediate hybridization step are required during PCR-cycling to allow cross-hybridization of mutant and WT alleles, making the reaction excessively long. In *fast*-COLD-PCR, the formation of heteroduplexes within the reaction is not required, thus the reaction is rapid and mutations are enriched anywhere along the sequence provided they result in an amplicon T_m that is lower than that of the WT sequence (T_m-reducing mutations, G:C > A:T or G:C > T:A). *Fast*-COLD-PCR results to enrichments of 10- to 100-fold, and is robust and time-efficient, but is limited to enriching only T_m-reducing mutations. The different capabilities of the two COLD-PCR formats pose a practical obstacle, since users have to decide in advance which of the COLD-PCR attributes they wish to utilize, thus reducing their options.

To combine the advantages of *full and fast* COLD-PCR in a single format, here we present an *ice* modification of the COLD-PCR technology. In order to enrich all mutation types, *ice*-COLD-PCR employs a reference sequence (RS) of a novel-design; the RS is engineered such that (i) it matches the WT-sequence of the anti-sense strand; (ii) PCR primers cannot bind to it; and (iii) it is phosphorylated on the 3′-end so that it is non-extendable by the polymerase (Figure 1). When incorporated into PCR reactions in excess relative to the template, the RS binds rapidly to the amplicons (Figure 1). At a critical denaturation temperature, the RS:WT duplexes remain double-stranded, thereby inhibiting selectively the
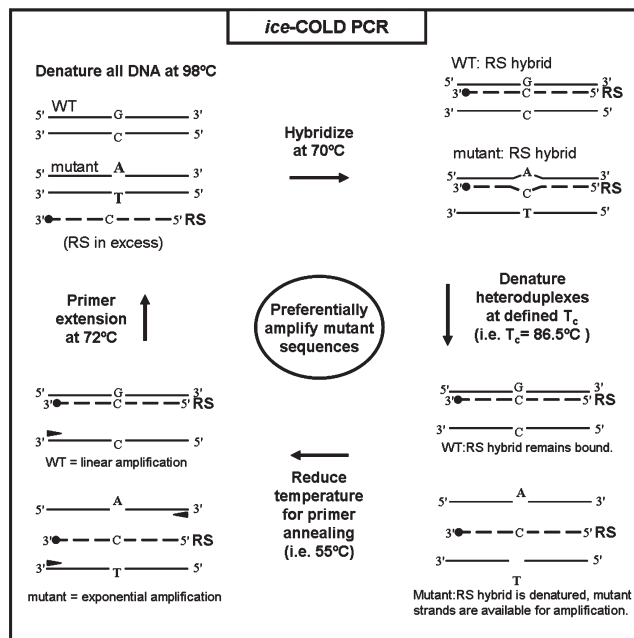

Figure 1. Schematic of *ice*-COLD-PCR. A RS (long oligonucleotide) was designed for each amplicon. Each RS is single-stranded, WT specific, complimentary to the sense strand, and contains a 3′-non-extensible phosphate group.

amplification of WT alleles throughout the thermocycling. Conversely, the RS:mutant duplexes are preferentially denatured and amplified. By using a WT-specific RS, all variants can be effectively amplified, regardless of mutational type and position. We demonstrate below that this novel *ice*-COLD-PCR platform removes shortcomings of previous COLD-PCR formats and allows for the efficient enrichment of complete mutational profiles. We present our findings from evaluations of serially diluted human cell-line DNA and genomic DNA from a human lung adenocarcinoma tumor specimen.

MATERIALS AND METHODS

Tumor specimens and genomic DNA

Human genomic DNA (male G1471, Promega Corporation, Madison, WI, USA) was employed as the WT control. Genomic DNA from human cancer cell-lines HCC2218 and HCC1008, which possess defined *TP53* mutations in exon 8 (Supplementary Table S1), was purchased from American Type Culture Collection. The human cell-line PFSK-1 was also purchased from ATCC Inc. (Manassas, VA, USA) and cultured; genomic DNA was extracted from cultured cells using a DNeasy™

Table 1. Oligonucleotide sequences for *ice*-COLD-PCR; sequence orientation is presented 5′–3′

Oligo	Target	Sequence (5′–3′)
RS1 (RS60)		
Ex8-167F[a]	167-bp amplicon	GCTTCTCTTTTCCTATCCTG
Ex8-167R[a]	167-bp amplicon	CTTACCTCGCTTAGTGCT
p53-87-F2[a]	87-bp amplicon	TGGTAATCTACTGGGACG
p53-87-R[a]	87-bp amplicon	CGGAGATTCTCTTCCTCT
30T-p53-87F	sequencing primer	TTTTTTTTTTTTTTTTTTTTTTTTTTTTTTTGGTAATCTACTGGGACG
60refseq-for	RS60 target region	GGACGGAACAGCTTT
60refseq-rev	RS60 target region	CTGGCCGCGTGTCTC
RS60	60 nt WT RS	CTCTGTGCGCCGGTCTCTCCCAGGACAGGCACAAACACGCACCT CAAAGCTGTTCCGTCC-phosphate
Nested-87F	Nested-pyroseq	TGGTAATCTACTGGGACG
Biotin-nested-87R	Biotinylated -pyroseq	Biotin-CGGAGATTCTCTTCCTCTGTG
RS-Pyro-Seq-primer	Sequencing primer	TGCCTGTCCTGGGAG
RS2 (RS90)		
Ex8-167F[a]	167-bp amplicon	GCTTCTCTTTTCCTATCCTG
Ex8-167R[a]	167-bp amplicon	CTTACCTCGCTTAGTGCT
p53-ex8-115F	115-bp amplicon	TTGCTTCTCTTTTCCTAT
p53-ex8-115R	115-bp amplicon	GCGGAGATTCTCTTC
40T-p53-115F	sequencing primer	TTTTTTTTTTTTTTTTTTTTTTTTTTTTTTTTTTTTTTTTGCTTCTCTTTTCCTATCC
90refseq-for	RS90 target region	CTTCCTCTGTGCGCC
90refseq-rev	RS90 target region	CTATCCTGAGTAGTG
RS90	90 nt WT RS	CTTCCTCTGTGCGCCGGTCTCTCCCAGGACAGGCACAAACACGCACCTCAAAG CTGTTCCGTCCCAGTAGATTACCACTACTCAGGATAG-phosphate

[a]Primers previously reported in ref. (9).

Blood and Tissue kit (Qiagen Inc., Valencia, CA, USA) per manufacturer's instructions.

One clinical lung adenocarcinoma tumor specimen, TL92, that was screened in a previous investigation (11) and found to contain a 1-bp heterozygous deletion in exon 8 (c.845del, p.Arg282del; Supplementary Table S1) was also selected for examination. TL92 belonged to a group of snap-frozen lung adenocarcinoma specimens obtained from the Massachusetts General Hospital Tumor Bank and used following Internal Review Board approval. Following manual macro-dissection, genomic DNA was isolated using the DNeasy™ Blood and Tissue kit (Qiagen Inc., Valencia, CA, USA). Genomic DNA concentration was quantified using a Nano-drop™ spectrophotometer.

Genomic DNA mixtures and conventional PCR amplification

To determine potential mutation enrichment, genomic DNA from human cell-lines HCC1008, HCC2218 and PFSK-1 and from lung adenocarcinoma specimen TL92 was serially diluted into WT DNA to generate an evaluation panel. The specific mutant DNA mixtures examined were: 10, 3, 1.0, 0.3 and 0.1% mutant-to-WT ratios. In addition, several replicates of WT DNA (0% mutant) were included and evaluated in parallel in each experiment.

Primers (Table 1) were designed to amplify a 167-bp region of TP53 exon 8 from genomic DNA in a conventional PCR reaction. The conventional PCR reactions were performed using 1× manufacturer-supplied HF (high fidelity) buffer, 1.5 mM MgCl$_2$, 0.2 mM dNTPs, 0.3 μM primers, 0.1× LCGreen+$^®$ dye, 5 U/μl Phusion™ high-fidelity polymerase (Finnzymes Inc.,

Woburn, MA, USA), and 50 ng of genomic DNA. The reactions were performed in real-time format, on a SmartCycler II (Cepheid Inc., Sunnyvale, CA, USA). Post-PCR melting and gel electrophoresis were performed to ensure specific amplification of the target amplicon. Thermocycling conditions are presented in Table 2. The 167-bp amplicon was subsequently used in nested PCR/COLD-PCR reactions that amplified two overlapping 87- and 115-bp PCR amplicons.

Reference sequences for *ice*-COLD-PCR

Two reference sequences (RS) of 60- and 90-nt long designed to enrich mutations within the 87- and 115-bp nested PCR amplicons (RS), respectively, were synthesized and HPLC-purified by Integrated DNA Technologies Inc. (Coralville, IA, USA). Each RS is an exact match to the WT amplicon, but somewhat shorter in length, such that the maximal overlap with the priming regions is ∼5 bp (Table 1). Each RS contains a 3′-non-extensible phosphate group to prevent extension by the polymerase throughout the course of PCR, Figure 1.

An RS can be designed to inhibit the amplification of either the sense or anti-sense strand of the WT allele. Preliminary investigations were performed to assess both a sense-strand RS and an anti-sense strand RS; both RS oligonucleotides functioned with equal efficiency (data not presented herein).

Initial evaluations were performed to determine the amount of RS molecules that were necessary to sufficiently inhibit amplification of the WT allele without adversely affecting the amplification. We amplified and compared RS concentrations ranging 0–100 nM (data not shown). For those conditions where amplification was

Table 2. PCR thermocycling conditions

PCR TYPE	STEP	CONDITIONS	T_c °C
Conventional PCR	Initial denaturation Thermocycling: 35 cycles	98°C for 30 s 98°C for 10 s T_a for 20 s 72°C for 10 s	N/A
	Melting Curve	Ramping 0.2°C/s, 65–98°C	
fast-COLD-PCR	Initial denaturation Stage 1 cycling: 5 cycles	98°C for 30 s 98°C for 10 s T_a for 20 s, fluorescent reading 72°C for 10 s	
	Stage 2 cycling: 20–35 cycles[a]	T_c for 10 s T_a for 20 s, fluorescent reading 72°C for 10 s	87 bp, $T_c = 85.5$°C 115 bp, $T_c = 85.4$°C
	Melting curve	Ramping 0.2°C/s, 65–98°C	
full-COLD-PCR	Initial denaturation Stage 1 cycling: 5 cycles	98°C for 30 s 98°C for 10 s T_a for 20 s, fluorescent reading 72°C for 10 s	
	Stage 2 cycling: 20–35 cycles[a]	98°C for 10 s 70°C for 30 s T_c for 10 s T_a for 20 s, fluorescent reading 72°C for 10 s	87 bp, $T_c = 85.5$°C 115 bp, $T_c = 85.4$°C
	Melting Curve	Ramping 0.2°C/s, 65–98°C	
ice-COLD-PCR	Initial denaturation Stage 1 cycling: 5 cycles	98°C for 30 s 98°C for 10 s T_a for 20 s, fluorescent reading 72°C for 10 s	
	Stage 2 cycling: 20-35 cycles[a]	98°C for 10 s 70°C for 30 s T_c for 10 s T_a for 20 s, fluorescent reading 72°C for 10 s	87 bp, $T_c = 84.1$°C 115 bp, $T_c = 83.4$°C
	Melting Curve	Ramping 0.2°C/s, 65–98°C	

T_a, annealing temperature; 60 and 55°C for the 87- and the 115-bp amplicons, respectively; T_c, Critical denaturation temperature used in COLD-PCR reactions.
[a]20 and 35 cycles were performed respectively for the 87-bp and the 115-bp amplicons.

reproducibly successful, the products were sequenced to determine the degree of enrichment achieved. We observed that 25 nM was an optimal RS concentration to allow PCR amplification of the mutant alleles to proceed efficiently while also effectively hybridizing to the WT strands. For all remaining assays, we used 25 nM RS in each ice-COLD-PCR reaction.

Determination of critical denaturation temperature, T_c

To define the critical denaturation temperatures (T_c) for both *full*- and *fast*-COLD-PCR of a given amplicon, a WT sample was first amplified via conventional PCR in the presence of an intercalating dye (LCGreen+, Idaho Technologies Inc., Salt Lake City, UT, USA), on a SmartCycler II (Cepheid Inc) real time PCR machine, followed by melting curve analysis (0.2°C/s, ramping 65–98°C), to identify the melting temperature (T_m). The T_c for *full*- and *fast*-COLD-PCR is typically 1°C below the experimentally-derived amplicon melting temperatures

(10). Defining the T_c in this empirical manner results to robust PCR amplification as well as substantial mutation enrichment. Because the critical denaturation temperature during COLD-PCR has to be controlled precisely (e.g. to within ± 0.2°C), it is important to use a thermocycler with high temperature precision. A SmartCycler II (Cepheid Inc.) was used in this investigation.

To determine the critical denaturation temperatures (T_c) for *ice*-COLD-PCR a modified procedure was used, as follows: RS engineered for *ice*-COLD-PCR are shorter than the PCR amplicon being evaluated (Figure 1), and as such the T_m of the RS differs from the T_m of amplicon. To determine the T_m of the RS, primers were designed such that an amplicon of the exact same length and sequence as the RS was amplified from WT DNA. Next, the RS–amplicon and the WT conventional PCR amplicon were mixed at the appropriate concentration, and followed by denaturation (98°C 30 s), hybridization (70°C 30 s), and a melting curve analysis to generate a T_m for the hybridized duplexes. Defining the critical denaturation temperature

(T_c) for *ice*-COLD-PCR at $1°C$ below the T_m of the RS–amplicon duplex was sufficient for mutation enrichment using either RS.

Analysis of *full*- and *ice*-COLD-PCR hybridization times and thermocycling conditions

Both *full*-COLD-PCR and *ice*-COLD-PCR thermocycling strategies include a hybridization step to allow cross-hybridization of mutant and WT alleles form heteroduplex molecules. Furthermore, in the original development of *full*-COLD-PCR (9), several minutes of an intermediate hybridization step (at $70°C$) was necessary to achieve optimal hybridization, making the reaction excessively long. In this evaluation, we employ a high-fidelity polymerase system, Phusion (Finnzymes, Inc.) and its respective proprietary buffer. Evaluations were performed to assess the optimal hybridization time for *full*-COLD-PCR and *ice*-COLD-PCR thermocycling using the Phusion polymerase system. Thermocycling conditions are presented in Table 2, however, the hybridization times were modified in each amplification platform (*full* and *ice*); for both thermocycling platforms, hybridization times of 10 s, 30 s, 1, 2 and 5 min were examined. A T_m-equivalent (HCC1008 cell-line DNA; c.841G > C, p.Asp281His), and a 3% T_m-increasing (PFSK-1 cell-line DNA, c.823T > G; p.Cys275Gly), 3% mutant:WT mixture was evaluated for each amplicon (87 and 115 bp). Amplicons were Sanger sequenced, and mutation abundance was assessed. After analysis [based on comparisons within this investigation, and comparison with previous studies (9)], a 30 s hybridization was determined to be the optimal hybridization time for both platforms, and was used in the remaining method development and assays.

Evaluation of ice-COLD-PCR and comparison to other forms of COLD-PCR

Using a 1:500 dilution of the 167-bp TP53 exon 8 amplicon as template, two 87- and 115-bp regions were amplified via nested PCR/COLD-PCR reactions and evaluated for low-abundance mutations. Four amplification strategies were followed: (i) conventional PCR, (ii) *full*-COLD-PCR, (iii) *fast*-COLD-PCR and (iv) *ice*-COLD-PCR. Mutant mixtures (10, 3, 1.0, 0.3 and 0.1%) were evaluated for each reaction type. *TP53* exon 8 was amplified using the primers presented in Supplementary Table S1.

Conventional PCR reactions were performed as described above for the 167-bp amplicon, however nested primers (Table 1) were used to generate 87- and 115-bp amplicons. Thermocycling conditions are as described above except that annealing temperatures were 60 and $55°C$ for each target region, respectively.

Full-COLD-PCR reactions were performed using $1×$ manufacturer-supplied HF (high fidelity) buffer, $1.5 mM$ $MgCl_2$, $0.2 mM$ dNTPs, $0.3 μM$ primers, $0.1×$ LCGreen+® dye (Idaho Technologies), $5 U/μl$ Phusion™ high fidelity polymerase (Finnzymes) and $1 μl$ diluted (1:500) 167-bp PCR amplicon. COLD-PCR was performed on a SmartCycler II (Cepheid Inc); *full*-COLD-PCR thermocycling included five initial PCR

cycles using a conventional denaturation temperature ($98°C$) to build-up the intended target amplicon from template DNA, and then continued using the critical denaturation temperature and a hybridization step with *full*-COLD-PCR reaction conditions. Thermocycling conditions are presented in Table 2.

Fast-COLD-PCR reactions were performed using reagent conditions as described above in the *full*-COLD-PCR section. All COLD-PCR reactions were performed on a SmartCycler II (Cepheid Inc). As in *full*-COLD-PCR, *fast*-COLD-PCR thermocycling included five initial PCR cycles using a conventional denaturation temperature ($98°C$) to build-up the intended target amplicon from template DNA, and then continued using the critical denaturation temperature with *fast*-COLD-PCR reaction conditions. Thermocycling conditions are presented in Table 2.

Ice-COLD-PCR reactions were performed in the presence of the appropriate RS, at $25 nM$ concentration. After determining the appropriate T_c for *ice*-COLD-PCR as described earlier, PCR amplification was performed on the mutant mixtures (10, 3, 1.0, 0.3 and 0.1% mutant) and WT control samples. *Ice*-COLD-PCR reactions were performed on the Cepheid SmartCycler II, using reagent conditions as described above in the *full*-COLD-PCR section and $25 nM$ RS. As in *full*-COLD-PCR, *ice*-COLD-PCR thermocycling included five initial PCR cycles using a conventional denaturation temperature ($98°C$) to build-up the intended target amplicon from template DNA, and then continued using the critical denaturation temperature and amplicon hybridization within the *ice*-COLD-PCR reaction conditions. Thermocycling conditions are presented in Table 2.

Sanger sequencing and pyrosequencing

Mutation enrichment via each PCR amplification approach was first evaluated by Sanger sequencing analysis. PCR/COLD-PCR products were subjected to digestion by exonuclease I (New England Biolabs, Ipswich, MA, USA) and shrimp alkaline phosphatase (USB Corporation, Cleveland, OH, USA) and sequenced at the Dana-Farber Cancer Institute, Molecular Biology Core Facility. Sequencing primers are presented in Table 1; due to the short length of the amplicons, a poly-T sequence was added to the 5′-end of the forward sequencing primer. Sequence chromatograms were evaluated using BioEdit™ biological sequence alignment editor (http://www.mbio.ncsu.edu/BioEdit/BioEdit.html). Approximate mutant nucleotide abundances, relative to the WT nucleotide, were calculated from the peak height values of the chromatograms.

Mutation enrichment was also evaluated via pyrosequencing analysis for selected samples. For pyrosequencing analysis, the 87-bp COLD-PCR/*ice*-COLD-PCR amplicons were amplified using 5′-biotinylated reverse primers (Table 1). A serial dilution (10, 3, 1, 0.3, 0.1 and 0%) of the HCC1008 T_m-equivalent mutation was evaluated. Amplicons were processed for pyrosequencing analysis at EpigenDx Inc. (Worcester, MA, USA). Mutant nucleotide abundances,

relative to the WT nucleotide, were calculated from the pyrophosphate peak height values of the pyrograms. Pyrograms were analyzed to compare the enrichment obtained via *full*-COLD-PCR and *ice*-COLD-PCR, and to determine the sensitivity of pyrosequencing compared to that of Sanger sequencing.

To assess variability and reproducibility, conventional and COLD-PCR reactions and sequencing evaluations were repeated independently, at least three times, on multiple days throughout several months, and were performed interchangeably within wells of two SmartCycler II (Cepheid) units.

RESULTS

Hybridization time and thermocycling protocols for *full*-COLD-PCR and ice-COLD-PCR

Evaluation of varying hybridization times (30 s–5 min) revealed that using Phusion high-fidelity polymerase (Finnzymes Inc.), and its proprietary buffer, that the originally determined extended hybridization step does not improve the enrichment, within either *full*-COLD-PCR or *ice*-COLD-PCR amplification (Supplementary Figures S1 and S2). Specifically, increasing the hybridization time from 30 s to 5 min does not appreciably influence the degree of enrichment. The 30-s hybridization time achieves higher enrichment than previously observed using the original *full*-COLD-PCR hybridization times with the alternative polymerase systems and buffers (9). Accordingly, the use of the Phusion polymerase and buffer presumably results in faster and more efficient hybridization of DNA strands during COLD-PCR and provides an improvement for *ice*-COLD-PCR as well as for *full*-COLD-PCR.

Evaluation of RS60, 87-bp amplicon

Four mutation types (T_m-increasing variant, T_m-equivalent variant, T_m-reducing variant and a T_m-reducing single-base deletion), at an initial 3% mutation abundance, were interrogated using the four PCR platforms (conventional, *full*-COLD-PCR, *fast*-COLD-PCR and *ice*-COLD-PCR). After amplification, Sanger sequence chromatograms were directly compared. *Ice*-COLD-PCR yielded ∼13-fold enrichment for T_m-increasing (Figure 2A; representative triplicate sequences are presented in Supplementary Figure S3) and T_m-equivalent mutations (Figure 2B; representative triplicate sequences are presented in Supplementary Figure S4), and ∼15-fold enrichment for T_m-reducing mutations (Figure 2C and D; representative triplicate sequences are presented in Supplementary Figures S5 and S6 for the T_m-reducing C > T mutation and the 1-bp [G] deletion in the lung adenocarcinoma specimen, respectively). *Full*-COLD-PCR demonstrated ∼5- to 8-fold enrichment for all mutations. Furthermore, *fast*-COLD-PCR, which can only enrich T_m-reducing mutations, exhibited ∼15- to 17-fold enrichment for these types of mutations, while the T_m-increasing and T_m-equivalent mutations remained undetectable. Regardless of mutant type and position, after *ice*-COLD-PCR amplification all mutation types

are strongly enriched and can be reliably identified in Sanger sequence chromatograms down to at least 1% mutation abundance (Supplementary Figure S7). While *full*-COLD-PCR exhibited the ability to modestly enrich each of the mutation types evaluated and assessed by Sanger sequencing analysis, the enrichment revealed by *ice*-COLD-PCR was significantly more pronounced (data for the 87-bp amplicon is presented in Figure 3). Furthermore, while *fast*-COLD-PCR was unable to enrich T_m-increasing and T_m-equivalent mutations, *ice*-COLD-PCR was efficient in enriching all mutation types including the single-base deletion (Figure 3).

As an alternative to Sanger sequencing chromatograms, pyrograms of *full*-COLD-PCR and *ice*-COLD-PCR amplicons of the serially diluted mutant mixtures were also compared (Figure 4). In the 87-bp amplicon, pyrosequencing analysis of *full*-COLD-PCR amplicons demonstrated moderate enrichment of the HCC1008 T_m-equivalent mutation. For example, in the pyrograms the 10% mutant-to-WT mixture appeared enriched by just >2-fold to ∼23%, after background subtraction. The mutation was detectable in serial dilution mixtures down to 1%, and demonstrated ∼3.5-fold enrichment to an abundance of 3.5% (Figure 4). Analysis of the pyrograms for *ice*-COLD-PCR exhibited higher levels of enrichment and sensitivity over *full*-COLD-PCR. After background subtraction, the 10% mixture, amplified by *ice*-COLD-PCR, presented a 5.5-fold increase to ∼55%. The mutation remained visible throughout the remaining serial dilution mixtures. The 1% mutant mixture amplified by *ice*-COLD-PCR exhibited ∼34-fold enrichment and the 0.1% mutant mixture, exhibited ∼75-fold enrichment.

Evaluation of RS90, 115-bp amplicon

The size of the sequence interrogated via *ice*-COLD-PCR is defined by the size of the RS. To evaluate *ice*-COLD-PCR for larger sequences, a 115-bp PCR amplicon combined with a 90-nt RS were examined next. The same four mutation types (T_{m}-increasing variant, T_{m}-equivalent variant, T_m-reducing variant, and a T_m-reducing deletion) were interrogated using the four PCR platforms (conventional, *full*-COLD, *fast*-COLD and *ice*-COLD-PCR). After amplification, Sanger sequence chromatograms were directly compared and evaluated. *Ice*-COLD-PCR yielded ∼13- to 15-fold enrichment for T_m-increasing and T_m-equivalent mutations (Supplementary Figure S8A), and ∼16-fold enrichment for T_m-reducing mutations. In contrast, *full*-COLD-PCR demonstrated ∼5- to 7-fold enrichment for T_m-increasing and T_m-equivalent mutations, and ∼10-fold for the T_m-reducing mutations (Supplementary Figure S8A). Furthermore, *fast*-COLD-PCR, which can only enrich T_m-reducing mutations, exhibited ∼16-fold enrichment for these types of mutations, while the T_m-increasing and T_m-equivalent mutations remained undetectable. Regardless of mutant type and position, after *ice*-COLD-PCR amplification, all mutation types are strongly enriched and can be reliably sequenced down to at least 1% mutation abundance (Supplementary Figure S8B).
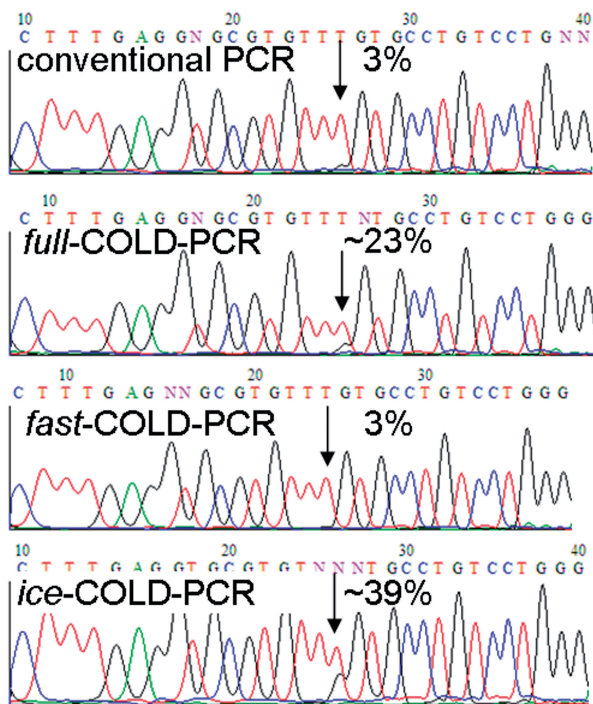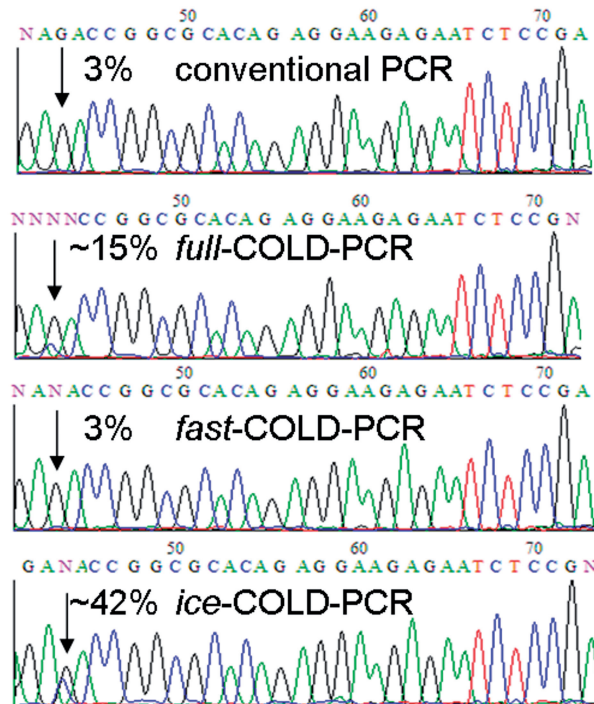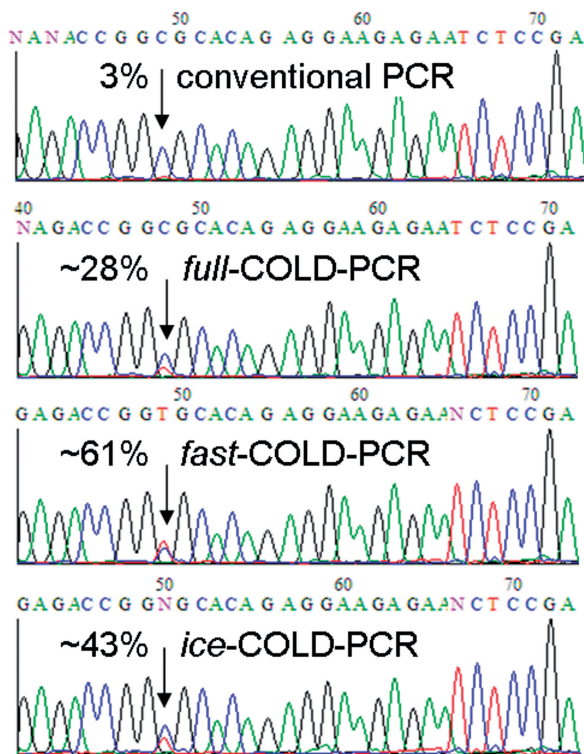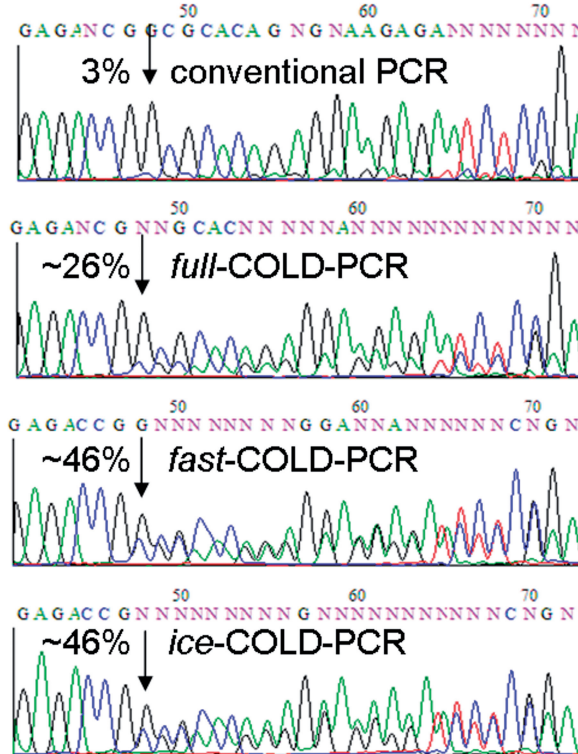
Figure 2. Comparison of a 87-bp PCR amplification approaches for (**A**) a low-abundance (3%) T_m-increasing mutation (PFSK-1 cell-line DNA, c.823T > G; p.Cys275Gly), (**B**) a low-abundance (3%) T_m-equivalent mutation (HCC1008 cell-line DNA; c.841G > C, p.Asp281His), (**C**) a low-abundance (3%) T_m-reducing mutation (HCC2218 cell-line DNA; c.847C > T, p.Arg283Cys) and (**D**) a low-abundance (3%) T_m-reducing one base pair deletion (c.845del, p.Arg282del) in DNA from a clinical lung adenocarcinoma specimen. Representative chromatograms are presented; estimates of fold improvement are based upon multiple evaluations.

DISCUSSION

The use of PCR-based enrichment methods is often necessary to elevate the mutant abundance to a level at which accurate and precise analysis is possible; however, it remains quite difficult to enrich for mutations that are unknown and at low-abundance. While there are many
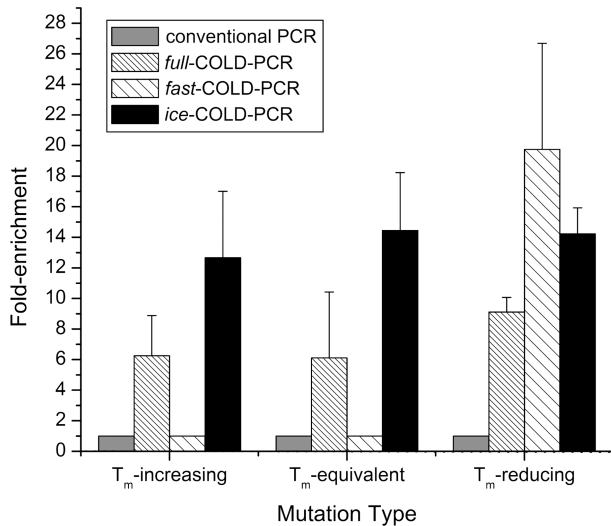
Figure 3. Fold-enrichment estimates for the 87-bp amplicon by PCR amplification platform for 3% abundance of a T_m-increasing (T > G), T_m-equivalent (G > C), and T_m-reducing (C > T) mutations after amplification by conventional PCR, *full*-COLD-PCR and *ice*-COLD-PCR, as analyzed by standard Sanger sequencing.

approaches to enrich low-abundance mutations of a known status and identity, there are very few methodologies capable of enriching and identifying all forms of unknown mutations (8,17,18). To detect low-abundance early mutations in tumors or the emergence of resistance mutations (e.g. at levels 10^{-3} to 10^{-6} mutant-to-WT DNA), both high selectivity and the enrichment of minority alleles is required for successful detection and identification. Furthermore, in order to use a particular approach as a routine diagnostic tool, there must be a balance of achieving high selectivity and enrichment while maintaining accuracy, convenience and low cost.

We demonstrated that the inclusion of long (60 or 90 nt) specially-designed oligonucleotides (RS) within COLD-PCR reactions selectively enhances denaturation of mutant over WT sequences throughout PCR, while also reducing time-intensive hybridization times. Our evaluations of the hybridization time at 70°C (30 s– 5 min) revealed that the use of the Phusion polymerase and proprietary buffer presumably results in faster and more efficient hybridization of DNA strands during COLD-PCR and provides an improvement for *ice*-COLD-PCR as well as for *full*-COLD-PCR.

The utilization of long sequences to improve differential denaturation of heteroduplexed versus homoduplexed sequences has not been attempted previously, and is distinct from the use of short, WT-blocking hybridization probes (19) or PNA/LNA-modified oligonucleotides that enrich
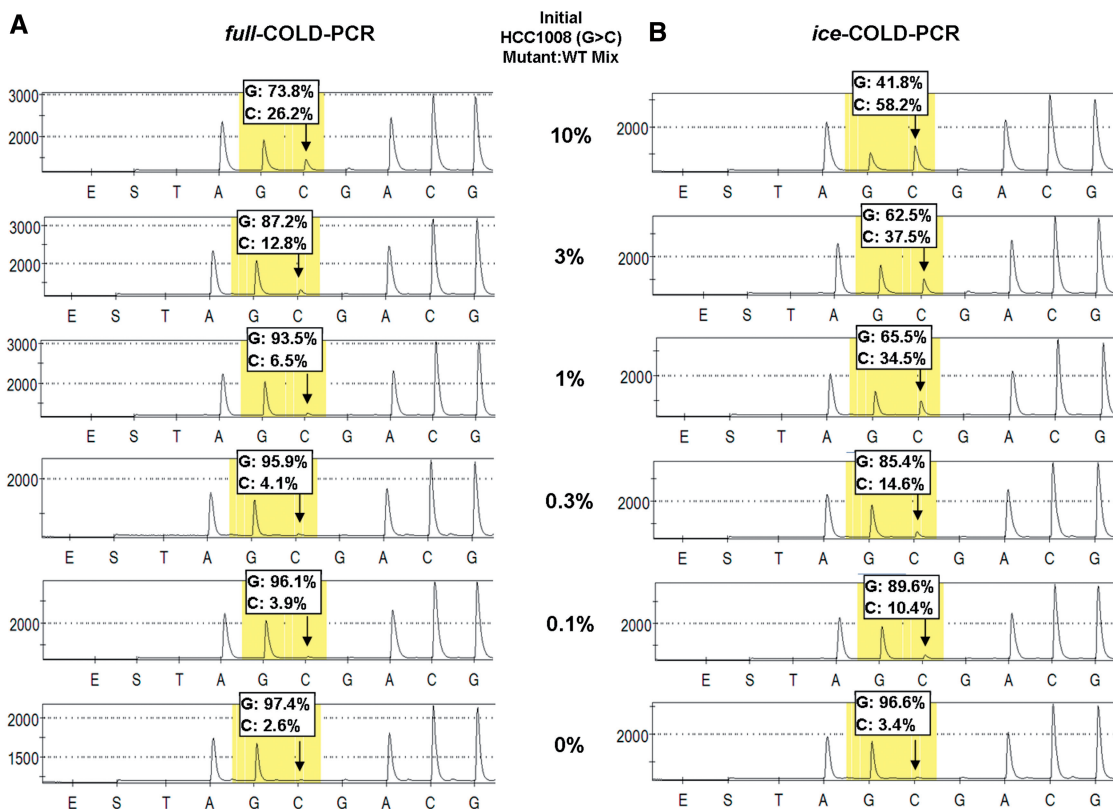
Figure 4. Pyrosequencing analysis of the 87-bp amplicon; pyrograms are presented for (**A**) *full*-COLD-PCR and (**B**) *ice*-COLD-PCR. Serial dilutions (3, 1, 0.3, 0.1 and 0%) of HCC1008 (c.841 G > C, p.Asp281His) in WT DNA are presented.

for specific mutations (20,21). It is also conceivable to introduce modified bases within a RS to improve selective denaturation even further during *ice*-COLD-PCR. Using an oligonucleotide synthesizer to construct the RS is convenient but has oligonucleotide-length limitations. Alternatively, longer RS can be synthesized using asymmetric PCR approaches, followed by end-modification of the single stranded DNA products.

We presented our evaluations of *ice*-COLD-PCR, in comparison with the other COLD-PCR platforms and conventional PCR, in serially diluted human cell-line genomic DNA as well as genomic DNA extracted from a human lung adenocarcinoma tumor specimen. Overall, the data indicate that *ice*-COLD-PCR provides a highly sensitive, rapid and economical approach for mutation enrichment, which simultaneously allows for direct sequencing for all types of unknown low-abundance mutations. While *fast*-COLD-PCR retains its edge in mutation enrichment, *ice*-COLD-PCR is most appropriate for use when the user is interested in examining all mutation types, particularly those that are unknown. Through the inclusion of a non-amplifying WT RS, *ice*-COLD-PCR demonstrates the ability to increase the mutational abundance >50% (relative to the WT allele); enrichment >50% cannot be achieved using *full*-COLD-PCR due to the unavoidable amplification of those WT alleles that form the heteroduplex with the mutant alleles. The data herein demonstrate that in addition to T_m-reducing mutations, low-abundance T_m-increasing and T_m-equivalent mutations can be enriched easily, robustly and rapidly via *ice*-COLD-PCR, and then subsequently identified through sequencing. The data also indicate that there is a clear sensitivity advantage to analyzing *ice*-COLD-PCR amplicons via pyrosequencing. While Sanger sequencing of *ice*-COLD-PCR amplicons demonstrated the ability to identify a 1% mutant, pyrosequencing allows the user to identify a 0.1% mutant mixture, demonstrating a 10-fold advantage in sensitivity based upon sequencing-methodology.

We observed an inverse relation in the enrichment potential relative to the initial mutation abundance, depending upon the type of mutant being enriched, the mutation abundance present in the un-amplified sample, and the sequencing method used for validation. For example, in Sanger sequencing chromatograms, 1% mutation abundances exhibited proportionally higher levels of enrichment (i.e. ~20-fold) than 10% mutant abundances (~4-fold); however, below 1% it remained difficult to identify the mutation fraction in Sanger sequence chromatograms. On the other hand, analysis of the 87-bp *ice*-COLD-PCR amplicons by pyrosequencing illustrates more clearly this inverse trend. For example, while the 10% mutant mixture exhibited ~5.5-fold enrichment, the 1% mutant mixture presented ~35-fold enrichment, and the 0.1% mutant mixture exhibited ~75-fold enrichment. This property suggests that COLD-PCR can potentially reveal mutations present at extremely low abundances in clinical specimens, especially when combined with sensitive downstream sequencing such as pyrosequencing or next generation sequencing. Thereby it may be possible to investigate the potential biological significance of traces of somatic mutations in cancer and mutator phenotypes (22).

Ice-COLD-PCR is expected to be beneficial in discerning the presence of intratumoral heterogeneity in clinical specimens, identifying the evolution of mutation spectra, and monitoring treatment response and disease progression. This approach may also be particularly valuable in detecting pre-cancerous genetic changes, screening mitochondrial DNA or DNA isolated from bodily fluids, defining tumor margins, and identifying mutations in cases where tumor cells are diffused within WT cells, such as in cancer formations in the pancreas and human airways (23). Applications of COLD-PCR in identifying fetal alleles in maternal circulation for pre-natal diagnosis have also been envisioned (24). In all such scenarios where mutations and variants are present at low-abundance, *ice*-COLD-PCR can be a powerful option for discrete enrichment of mutational events, such that downstream mutational identification becomes feasible.

CONCLUSIONS

In conclusion, we have developed *ice*-COLD-PCR, an advantageous platform appropriate for the discovery and identification of low-abundance unknown mutations and allele-variants. The inclusion of an appropriately designed RS within COLD-PCR selectively inhibits WT amplification throughout PCR, while preferentially enriches mutants and reducing time-intensive hybridization times. *Ice*-COLD-PCR combines high sensitivity, speed and ease of use, and facilitates direct sequencing for all types of unknown low-abundance mutations in clinical cancer specimens. Identifying and discerning the clinical significance of low-abundance mutations will have a profound influence on our understanding of cancer origin, evolution, risk, recurrence and treatment diagnostics.

SUPPLEMENTARY DATA

Supplementary Data are available at NAR Online.

ACKNOWLEDGEMENTS

FUNDING

REFERENCES

1. Kobayashi,S., Boggon,T.J., Dayaram,T., Janne,P.A., Kocher,O., Meyerson,M., Johnson,B.E., Eck,M.J., Tenen,D.G. and Halmos,B. (2005) EGFR mutation and resistance of non-small-cell lung cancer to gefitinib. *N. Engl. J. Med.*, **352**, 786–792.

2. Sjoholm,M.I.L., Hoffmann,G., Lindgren,S., Dillner,J. and Carlson,J. (2005) Comparison of archival plasma and formalin-fixed paraffin-embedded tissue for genotyping in hepatocellular carcinoma. *Cancer Epidemiol. Biomarkers Prevention*, **14**, 251–255.

3. Barcellos,L.F., Klitz,W., Field,L.L., Tobias,R., Bowcock,A.M., Wilson,R., Nelson,M.P., Nagatomi,J. and Thomson,G. (1997) Association mapping of disease loci, by use of a pooled DNA genomic screen. *Am. J. Hum. Genet.*, **61**, 734–747.

4. Fukui,T., Ohe,Y., Tsuta,K., Furuta,K., Sakamoto,H., Takano,T., Nokihara,H., Yamamoto,N., Sekine,I., Kunitoh,H. *et al.* (2008) Prospective study of the accuracy of EGFR mutational analysis by high-resolution melting analysis in small samples obtained from patients with non-small cell lung cancer. *Clin. Cancer Res.*, **14**, 4751–4757.

5. Shah,S.P., Morin,R.D., Khattra,J., Prentice,L., Pugh,T., Burleigh,A., Delaney,A., Gelmon,K., Guliany,R., Senz,J. *et al.* (2009) Mutational evolution in a lobular breast tumour profiled at single nucleotide resolution. *Nature*, **461**, 809–813.

6. Prat,E., del Rey,J., Camps,J., Ponsa,I., Lloreta,J., Egozcue,J., Gelabert,A., Campillo,M. and Miro,R. (2008) Genomic imbalances in urothelial cancer: Intratumor heterogeneity versus multifocality. *Diagn. Mol. Pathol.*, **17**, 134–140.

7. Sidransky,D. (2002) Emerging molecular markers of cancer. *Nat. Rev. Cancer*, **2**, 210–219.

8. Milbury,C.A., Li,J. and Makrigiorgos,G.M. (2009) PCR-based methods for the enrichment of minority alleles and mutations. *Clin. Chem.*, **55**, 632–640.

9. Li,J., Wang,L., Mamon,H., Kulke,M.H., Berbeco,R. and Makrigiorgos,G.M. (2008) Replacing PCR with COLD-PCR enriches variant DNA sequences and redefines the sensitivity of genetic testing. *Nat. Med.*, **14**, 579–584.

10. Milbury,C.A., Li,J. and Makrigiorgos,G.M. (2009) COLD-PCR-enhanced high-resolution melting enables rapid and selective identification of low-level unknown mutations. *Clin. Chem.*, **55**, 2130–2143.

11. Li,J., Milbury,C.A., Li,C. and Makrigiorgos,G.M. (2009) Two-round coamplification at lower denaturation temperature-PCR (COLD-PCR)-based sanger sequencing identifies a novel spectrum of low-level mutations in lung adenocarcinoma. *Hum. Mutat.*, **30**, 1583–1590.

12. Li,J., Wang,L., Janne,P.A. and Makrigiorgos,G.M. (2009) Coamplification at lower denaturation temperature-PCR increases mutation-detection selectivity of TaqMan-based real-time PCR. *Clin. Chem.*, **55**, 748–756.

13. Maekawa,M., Taniguchi,T., Hamada,E. and Takeshita,A. (2009) Efficiency of COLD-PCR for enrichment of K-ras mutation; a proof by use of SSCP analysis. *Clin. Chem.*, **55**, A219–A219.

14. Delaney,D., Diss,T.C., Presneau,N., Hing,S., Berisha,F., Idowu,B.D., O'Donnell,P., Skinner,J.A., Tirabosco,R. and Flanagan,A.M. (2009) GNAS1 mutations occur more commonly than previously thought in intramuscular myxoma. *Modern Pathol.*, **22**, 718–724.

15. Mancini,I., Santucci,C., Sestini,R., Simi,L., Pratesi,N., Cianchi,F., Valanzano,R., Pinzani,P. and Orlando,C. (2010) The use of COLD-PCR and high-resolution melting analysis improves the limit of detection of KRAS and BRAF mutations in colorectal cancer. *J. Mol. Diagn.*, **12**, 705–711.

16. Luthra,R. and Zuo,Z. (2009) COLD-PCR finds hot application in mutation analysis. *Clin. Chem.*, **55**, 2077–2078.

17. Parsons,B.L. and Heflich,R.H. (1997) Genotypic selection methods for the direct analysis of point mutations. *Mutat. Res.*, **387**, 97–121.

18. Gocke,C.D., Benko,F.A., Kopreski,M.S. and Evans,D.B. (2000) *Circulating Nucleic Acids in Plasma or Serum*, Vol. 906. New York Academy of Sciences, NY, pp. 31–38.

19. Liew,M., Nelson,L., Margraf,R., Mitchell,S., Erali,M., Mao,R., Lyon,E. and Wittwer,C. (2006) Genotyping of human platelet antigens 1 to 6 and 15 by high-resolution amplicon melting and conventional hybridization probes. *J. Mol. Diagn.*, **8**, 97–104.

20. Dean,F.B., Hosono,S., Fang,L., Wu,X., Faruqi,A.F., Bray-Ward,P., Sun,Z., Zong,Q., Du,Y., Du,J. *et al.* (2002) Comprehensive human genome amplification using multiple displacement amplification. *Proc. Natl Acad. Sci. USA*, **99**, 5261–5266.

21. Amicarelli,G., Adlerstein,D., Shehi,E., Wang,F.F. and Makrigiorgos,G.M. (2006) Genotype-specific signal generation based on digestion of 3-way DNA junctions: application to KRAS variation detection. *Clin. Chem.*, **52**, 1855–1863.

22. Loeb,L.A. (1991) Mutator phenotype may be required for multistage carcinogenesis. *Cancer Res.*, **51**, 3075–3079.

23. Park,I.W., Wistuba,II., Maitra,A., Milchgrub,S., Virmani,A.K., Minna,J.D. and Gazdar,A.F. (1999) Multiple clonal abnormalities in the bronchial epithelium of patients with lung cancer. *J. Natl Cancer Inst.*, **91**, 1863–1868.

24. Pinzani,P., Salvianti,F., Pazzagli,M. and Orlando,C. (2010) Circulating nucleic acids in cancer and pregnancy. *Methods*, **50**, 302–307.